

# Fabrication of 150-nm T-Gate Metamorphic AlInAs/GaInAs HEMTs on GaAs Substrates by MOCVD

Haiou Li, Zhihong Feng, Chak Wah Tang, and Kei May Lau

**Abstract**—Metamorphic AlInAs/GaInAs high-electron-mobility transistors (HEMTs) of 150-nm gate length with very good device performance have been grown by metal–organic chemical vapor deposition, with the introduction of an effective multistage buffering scheme. By using a combined optical and e-beam photolithography technology, submicrometer mHEMT devices have been achieved. The devices exhibit good dc and RF performance. The maximum transconductance was 1074 mS/mm. The nonalloyed ohmic contact resistance  $R_c$  was as low as  $0.02 \Omega \cdot \text{mm}$ . The unity current gain cutoff frequency ( $f_T$ ) and the maximum oscillation frequency ( $f_{\text{max}}$ ) were 279 and 231 GHz, respectively. This device has the highest  $f_T$  yet reported for 150-nm gate-length HEMTs. Also, an input capacitance to gate–drain feedback capacitance ratio  $C_{gs}/C_{gd}$  of 3.2 is obtained in the device.

**Index Terms**—AlInAs/GaInAs, GaAs, metal–organic chemical vapor deposition (MOCVD), metamorphic high-electron-mobility transistors (mHEMTs).

## I. INTRODUCTION

IN RECENT years, there has been an intense interest in the fabrication of GaAs-based high-speed devices for digital and microwave applications by molecular beam epitaxy (MBE) or metal–organic chemical vapor deposition MOCVD. HEMTs based on the lattice-matched InAlAs/InGaAs/InP material system have demonstrated the highest unity current gain cutoff frequency and the highest maximum frequency of oscillation for any transistor [1]. However, although InP-based devices have been shown to have superior performance in higher frequency and power applications, the InP industry has not experienced similar demand and growth. The downturn of the photonics industry, a major driving force behind the InP-based devices and circuits, did not help. Without large-volume consumption, the cost of InP substrates and chip manufacturing remains very expensive, making InP-based devices less competitive in the market place.

Manuscript received May 9, 2011; revised June 4, 2011; accepted June 8, 2011. This work was supported in part by the Research Grants Council of Hong Kong under CERG Grant 615506, by Intel Corporation, and by the National Natural Science Foundation of China under Grant 60876009. The review of this letter was arranged by Editor G. Meneghesso.

H. Li is with the School of Information and Communication, Guilin University of Electronic Technology, Guilin 541004, China, and also with the Department of Electronic and Computer Engineering, Hong Kong University of Science and Technology, Kowloon, Hong Kong.

Z. Feng is with Science and Technology on ASIC Laboratory, Hebei Semiconductor Research Institute, Shijiazhuang 050051, China.

C. W. Tang and K. M. Lau are with the Department of Electronic and Computer Engineering, Hong Kong University of Science and Technology, Kowloon, Hong Kong (e-mail: eekmlau@ust.hk).

Digital Object Identifier 10.1109/LED.2011.2159824

The emergence of metamorphic devices in the past few years shed light on this new approach of improving RF device performance at a lower cost. There are different buffering schemes on GaAs substrate allowing the growth of structure for high-quality RF devices traditionally grown on InP substrates. MBE has been extremely successful in developing metamorphic technology. There have been many reports on mHEMTs and mHBTs grown by MBE, with device results comparable to those on InP substrates [2], [3]. Metamorphic technology by MOCVD lags behind. There are many technological challenges to be overcome due to the large density of threading dislocation defects in the epilayers resulting from the lattice mismatch and difference in thermal expansion coefficient between GaAs substrate and grown layers. Although growth of structures for RF devices by MOCVD has always been at a slower development pace than MBE, the commercial success of few epitaxial material suppliers using MOCVD demonstrated the manufacturing advantages of MOCVD. One of the difficulties of growing metamorphic RF devices by MOCVD is to suppress the buffer leakage. Slight buffer leakage tends to degrade the RF operation of HEMTs with parasitic components [4]. With a 4% lattice mismatch between InP and GaAs, the common metamorphic growth technique is to grow a thick buffer with graded alloy compositions or super lattices. Unintentional impurities incorporated in these layers decrease the resistivity of the buffer, resulting in devices that cannot be pinched off. We have developed a growth technique of a comparatively thin multistage buffer to obtain high resistivity in the buffer layer leading to good device performance. This sets the stage for potential high-volume production of mHEMTs by MOCVD.

## II. MATERIAL GROWTH AND DEVICE FABRICATION

The wafers were grown by MOCVD on 4-in (001) oriented semi-insulating GaAs substrates in an Aixtron AIX-200/4 MOCVD system. The composite buffer stack consists of a low-temperature (LT) InP nucleation layer (110 nm), high-temperature (HT) undoped InP (650 nm) as buffer 1, LT-InP:C (100 nm) as buffer 2, and undoped LT- $\text{Al}_{0.49}\text{In}_{0.51}\text{As}$  (200 nm) and HT- $\text{Al}_{0.49}\text{In}_{0.51}\text{As}$  (100 nm) as buffer 3 and buffer 4, respectively; A 25-nm undoped  $\text{Ga}_{0.47}\text{In}_{0.53}\text{As}$  channel was grown on the buffer layer and is followed by a 5-nm undoped  $\text{Al}_{0.49}\text{In}_{0.51}\text{As}$  spacer layer, a Si-doping plane, a 25-nm undoped  $\text{Al}_{0.49}\text{In}_{0.51}\text{As}$  Schottky contact layer, and a 15-nm  $\text{Ga}_{0.47}\text{In}_{0.53}\text{As}$  cap layer. The metamorphic layer structures grown on GaAs substrates have been characterized and demonstrated with good electrical properties in our previous works [5], [6]. With the cap layer removed, a room-temperature

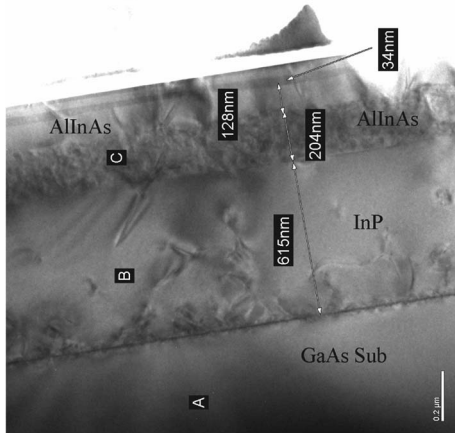


Fig. 1. TEM cross-sectional micrograph of AlInAs/GaInAs GaAs-mHEMT.

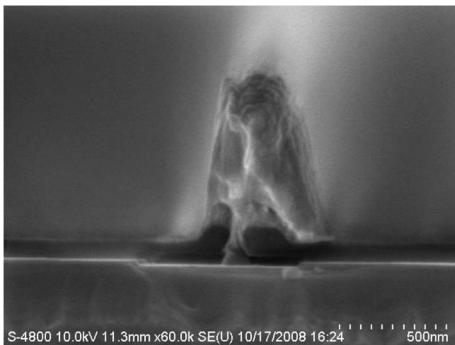


Fig. 2. Cross-sectional SEM graph of 150-nm T-shaped gate mHEMTs.

2DEG electron concentration of  $4.6 \times 10^{12} \text{ cm}^{-2}$  and a mobility of  $8740 \text{ cm}^2/\text{V}\cdot\text{s}$  were measured for this heterostructure. The sheet resistance of the mHEMT wafer is  $156 \text{ } \Omega/\text{sq}$ . The LT grown InP:C and InAlAs show high sheet resistivity, greater than  $10^5 \text{ } \Omega/\text{sq}$ . The root mean square (rms) value of the surface roughness is  $2.9 \text{ nm}$  across a scan area of  $20 \times 20 \text{ } \mu\text{m}^2$ . Fig. 1 shows a cross-sectional TEM micrograph of the whole structure including the multistage buffer and the mHEMT epilayer. In the photograph, the interfaces of all layers are clearly shown, and the thickness of each layer is in fair agreement with the designed structure. A, B, and C means GaAs, InP, and AlInAs buffer layers. Some  $60^\circ$  threading dislocations could be observed in the composite buffer.

The devices were fabricated with mesa isolation and six-layer metal system (Ni/Ge/Au/Ge/Ni/Au) ohmic contacts. Using the transmission line model, the nonalloyed ohmic contact resistance  $R_c$  was as low as  $0.02 \text{ } \Omega \cdot \text{mm}$ , which is due to higher doping concentration of cap layer and optimization of ohmic contact metal systems. T-gate devices of  $150 \text{ nm}$  were fabricated by a two-stage electron beam lithography process as shown in Fig. 2.  $\text{SiO}_2$  ( $10 \text{ nm}$ ) and  $\text{SiN}_x$  ( $100 \text{ nm}$ ) films were deposited by PECVD to define the gate footprint and to mechanically support the T-shaped gate. After etching of the  $\text{SiN}_x$  film with  $\text{CF}_4/\text{O}_2$  reactive ion etching, the gate-head pattern was formed by a bilayer PMMA/P(MMA-MAA) process. The high selectively citric-acid-based etchant was used to remove the highly doped GaInAs cap layer in order to stack T-shaped gates on the AlInAs barrier layer. Finally, Ti/Pt/Au was deposited as the Schottky gate contact.

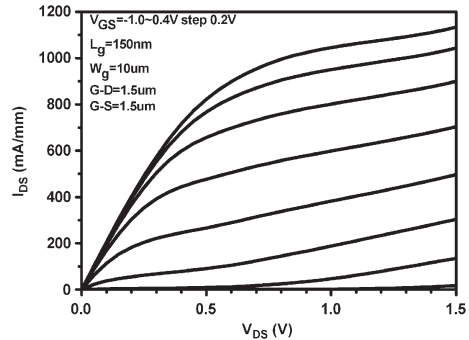
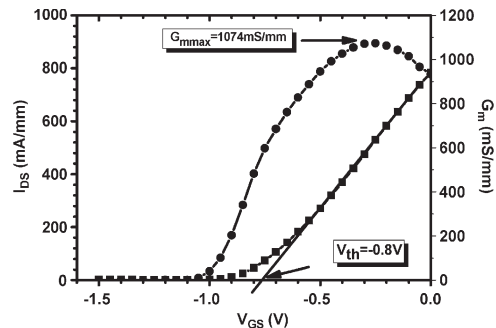
Fig. 3. DC  $I$ - $V$  characteristics of 150-nm mHEMT.

Fig. 4. Transfer characteristics of 150-nm mHEMT.

### III. DC CHARACTERISTICS

DC characterization of the  $150\text{-nm}$  gate-length mHEMTs was performed using an Agilent 4155 semiconductor parameter analyzer. The dc current-voltage characteristics of a typical AlInAs/GaInAs mHEMT with  $150\text{-nm}$  gate length are shown in Fig. 3. The maximum drain current measured at  $V_{GS} = 0.4 \text{ V}$  and  $V_{DS} = 1.5 \text{ V}$  was  $1130 \text{ mA/mm}$ . Fig. 4 shows the transfer characteristics. The maximum extrinsic transconductance is  $1074 \text{ mS/mm}$  at  $V_{GS} = -0.25 \text{ V}$  and  $V_{DS} = 1.0 \text{ V}$ . The device is a depletion-mode transistor with a threshold voltage  $V_{th}$  of around  $-0.8 \text{ V}$ . The threshold voltage of mHEMT device was not uniform, which shifts from  $-1.0$  to  $-0.8 \text{ V}$  due to larger surface roughness ( $rms > 2.9 \text{ nm}$ , as across a scan area of  $20 \times 20 \text{ } \mu\text{m}^2$ ). It will be further improved by optimizing the growth of mHEMT material. The device with composite buffer stack growth exhibited good pinchoff characteristics and little buffer leakage current, which will be further improved by optimizing the growth of buffer layer.

### IV. RF PERFORMANCE

On-wafer RF measurements were carried out on a  $150 \text{ nm} \times 100 \text{ } \mu\text{m}$  mHEMT using a Cascade Microtech probe station and an HP8722 network analyzer from  $0.1$  to  $39.9 \text{ GHz}$ . Open on-wafer deembedding structures were used to determine the parasitic capacitance of the probe pads and to deembed the short-circuit current gain  $|h_{21}|$ . The cutoff frequency  $f_T$  was obtained from the extrapolation of  $|h_{21}|$  to unity by using a  $-20 \text{ dB/dec}$  slope, and the maximum frequency of oscillation  $f_{max}$  was extrapolated from the MSG/MAG. Fig. 5 shows the current gain and MSG/MAG as a function of frequency.  $f_T$  is  $279 \text{ GHz}$ , which is the highest  $f_T$  yet reported for similar device, and  $f_{max}$  is  $231 \text{ GHz}$ . The optimum bias condition for

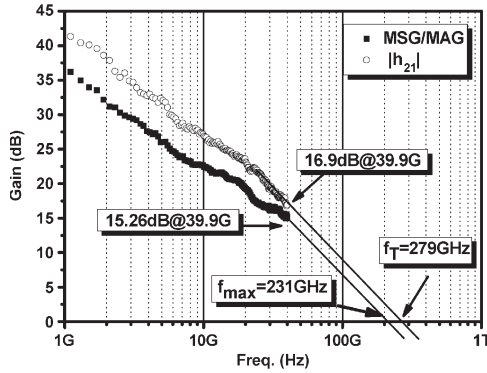


Fig. 5. Current gain and MSG/MAG as a function of frequency for 150-nm mHEMT.

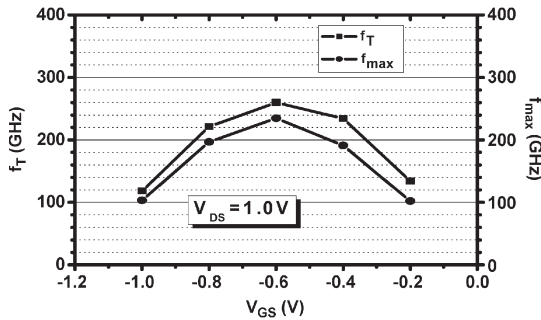


Fig. 6. Dependences of  $f_T$  and  $f_{max}$  on gate bias for 150-nm mHEMTs, where  $V_{DS}$  is fixed at 1.0 V.

TABLE I  
COMPARISON OF AlInAs/GaInAs HEMT PERFORMANCE

Hetero-structure	Sub.	Grow th	Mob.	Lg (nm)	Gm(mS/mm)	$f_T$ (GHz)	$f_{max}$ (GHz)	Date.	Ref.
In <sub>0.53</sub> GaAs/In <sub>0.52</sub> AlAs	GaAs	MBE	N/A	100	750	154	300	2004	[7]
InGaAs/InAlAs	GaAs	MBE	N/A	100	690	189	334	2004	[8]
In <sub>0.53</sub> GaAs/In <sub>0.52</sub> AlAs	GaAs	MBE	9100	150	740	150	240	2003	[9]
InGaAs/InAlAs	InP	MBE	8800	150	800	151	172	2006	[10]
In <sub>0.4</sub> GaAs/In <sub>0.35</sub> AlAs	GaAs	MBE	7650	100	700	210	N/A	2005	[11]
In <sub>0.53</sub> GaAs/In <sub>0.52</sub> AlAs	GaAs	MOCVD	8740	150	1074	279	231	2010	HK PTC

TABLE II  
SMALL-SIGNAL EQUIVALENT CIRCUIT MODEL  
PARAMETERS OF 150-nm mHEMTs

$C_{gs}$	$C_{gd}$	$G_m$	$G_{ds}$	$C_{gs}/C_{gd}$	$G_m/G_{ds}$
27.7fF	8.73fF	107mS	14.8mS	3.2	7.3

maximum unity current gain cutoff frequency is determined to be  $V_{GS} = -0.6$  V and  $V_{DS} = 1.0$  V. The dependences of  $f_T$  and  $f_{max}$  on the gate bias are shown in Fig. 6.  $f_T$  is relatively constant at both low and high gate biases, indicating a good linearity.

Table I shows the comparison of different AlInAs/GaInAs HEMT performances, which were grown by MBE or MOCVD on GaAs or InP substrates with similar gate-length HEMTs. The performance of mHEMTs grown by MOCVD is comparable to that of HEMT technology grown by MBE. These results are very encouraging toward the manufacturing of metamorphic devices on GaAs substrates by MOCVD. In this report, 150-nm

gate-length mHEMT has the highest  $f_T$ , due to the optimization of composite buffer stack growth and process.

We also analyzed the input capacitance to gate–drain feedback capacitance ratio  $C_{gs}/C_{gd}$  and voltage gain  $G_m/G_{ds}$  as shown in Table II. They are very important RF parameters and have a strong influence on the value of  $f_{max}$ .  $C_{gs}/C_{gd}$  and  $G_m/G_{ds}$  were determined by equivalent circuit modeling of measured 10–30-GHz S-parameters ( $V_{GS} = -0.6$  V and  $V_{DS} = 1.0$  V). The device has an output conductance ( $G_{ds}$ ) of 14.8 mS, and  $G_m/G_{ds}$  is 7.3. The input capacitance to gate–drain feedback capacitance ratio  $C_{gs}/C_{gd}$  is 3.2.

## V. CONCLUSION

In conclusion, we have successfully grown metamorphic AlInAs/GaInAs HEMTs with good device performance by using the MOCVD technique through the introduction of a multistage buffer. A depletion-mode mHEMT exhibits the maximum transconductance of 1074 mS/mm. With 150-nm gate-length devices,  $f_T$  and  $f_{max}$  of 279 and 231 GHz, respectively, were obtained. The result is comparable to the structure of mHEMT grown by MBE. We believe that these results are the best reported for MOCVD-grown mHEMTs and sufficient for high-frequency high-speed applications. With the anticipated demand of commercial high-speed and high-performance transistors, mHEMT technology by MOCVD is very attractive for manufacturing.

## REFERENCES

- [1] Y. Yamashita, A. Endoh, K. Shinohara, K. Hikosaka, T. Matsui, S. Hiyamizu, and T. Mimura, "Pseudomorphic In<sub>0.52</sub>Al<sub>0.48</sub>As/In<sub>0.7</sub>Ga<sub>0.3</sub> as HEMTs with an ultrahigh  $f_T$  of 562 GHz," *IEEE Electron Device Lett.*, vol. 23, no. 10, pp. 573–575, Oct. 2002.
- [2] W. E. Hoke, T. D. Kennedy, A. Torabi, C. S. Whelan, P. F. Marsh, R. E. Leoni, C. Xu, and K. C. Hsieh, "High indium metamorphic HEMT on a GaAs substrate," *J. Cryst. Growth*, vol. 251, no. 1–4, pp. 827–831, Apr. 2003.
- [3] M. Washima, T. Tanaka, and T. Hashimoto, "MOVPE grown metamorphic HEMT epitaxial wafers," *Hitachi Cable Rev.*, no. 20, pp. 39–44, 2001.
- [4] W.-C. Hsu, D.-H. Huang, Y.-S. Lin, Y.-J. Chen, J.-C. Huang, and C.-L. Wu, "Performance improvement in tensile-strained In<sub>0.5</sub>Al<sub>0.5</sub>As/In<sub>x</sub>Ga<sub>1-x</sub>As/In<sub>0.5</sub>Al<sub>0.5</sub>As metamorphic HEMT," *IEEE Trans. Electron Devices*, vol. 53, no. 3, pp. 406–412, Mar. 2006.
- [5] H. O. Li, C. W. Tang, K. J. Chen, and K. M. Lau, "Enhancement-mode metamorphic InAlAs/InGaAs HEMTs on GaAs substrates with reduced leakage current by CF<sub>4</sub> plasma treatment," in *Proc. CS Mantech Conf.*, May 2007, pp. 313–315.
- [6] H. O. Li, C. W. Tang, K. J. Chen, and K. M. Lau, "Metamorphic InAlAs/InGaAs HEMTs on GaAs substrates grown by MOCVD," *IEEE Electron Device Lett.*, vol. 29, no. 6, pp. 561–564, Jun. 2008.
- [7] Y. C. Lien, E. Y. Chang, H. C. Chang, L. H. Chu, G. W. Huang, H. M. Lee, C. S. Lee, S. H. Chen, P. T. Shen, and C. Y. Chang, "Low-noise metamorphic HEMTs with reflowed 0.1- $\mu$ m T-gate," *IEEE Electron Device Lett.*, vol. 25, no. 6, pp. 348–350, Jun. 2004.
- [8] B.-H. Lee, D. An, M.-K. Lee, B.-O. Lim, S.-D. Kim, and J.-K. Rhee, "Two-stage broadband high-gain W-band amplifier using 0.1- $\mu$ m metamorphic HEMT technology," *IEEE Electron Device Lett.*, vol. 25, no. 12, pp. 766–768, Dec. 2004.
- [9] H. S. Yoon, J. H. Lee, J. Y. Shim, J. Y. Hong, D. M. Kang, W. J. Chang, H. C. Kim, and K. I. Cho, "0.15  $\mu$ m gate length InAlAs/InGaAs power metamorphic HEMT on GaAs substrate with extremely low noise characteristics," in *Proc. 16th Int. Conf. Indium Phosphide Relat. Mater.*, May 2003, pp. 114–117.
- [10] S. Kim and I. Adesida, "0.15- $\mu$ m-gate InAlAs/InGaAs/InP E-HEMTs utilizing Ir/Ti/Pt/Au gate structure," *IEEE Electron Device Lett.*, vol. 27, no. 11, pp. 873–876, Nov. 2006.
- [11] S.-W. Kim, K.-M. Lee, J.-H. Lee, and K.-S. Seo, "High-performance 0.1- $\mu$ m In<sub>0.4</sub>AlAs/In<sub>0.35</sub>GaAs MHEMTs with Ar plasma treatment," *IEEE Electron Device Lett.*, vol. 26, no. 11, pp. 787–789, Nov. 2005.